Science of the Total Environment 746 (2020) 141139

Contents lists available at ScienceDirect

Science of the Total Environment

journal homepage: www.elsevier.com/locate/scitotenv

Impacts of human disturbance on the biogeochemical nitrogen cycle in a subtropical river system revealed by nitrifier and denitrifier genes

Jingjie Lin [a], Nengwang Chen [a,b,*], Xin Yuan [a], Qing Tian [a], Anyi Hu [c], Yi Zheng [d]

[a] Fujian Provincial Key Laboratory for Coastal Ecology and Environmental Studies, College of the Environment and Ecology, Xiamen University, Xiamen, China
[b] State Key Laboratory of Marine Environment Science, Xiamen University, Xiamen, China
[c] CAS Key Laboratory of Urban Pollutant Conversion, Institute of Urban Environment, Chinese Academy of Sciences, Xiamen, China
[d] Guangdong Provincial Key Laboratory of Soil and Groundwater Pollution Control, School of Environmental Science and Engineering, Southern University of Science and Technology, Shenzhen, China

HIGHLIGHTS

- AOB was dominant in the urban river section while AOA dominated in the agriculture river section
- Warm climate and large TSM in the wet season promote the growth of nitrifiers and denitrifiers
- Potential N retention by gaseous removal in the urban river section and reservoirs was higher

GRAPHICAL ABSTRACT

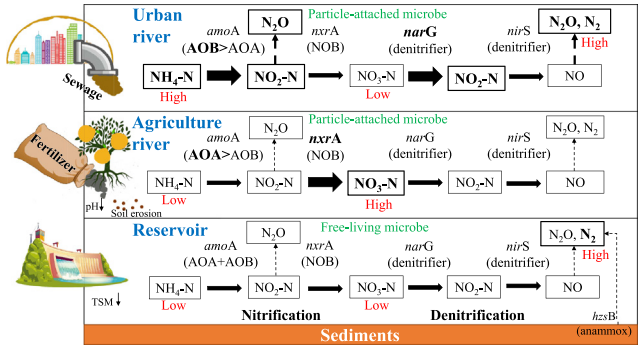

ARTICLE INFO

Article history:
Received 11 February 2020
Received in revised form 15 July 2020
Accepted 19 July 2020
Available online 22 July 2020

Editor: Sergi Sabater

Keywords:
Nitrification
Denitrification
Nitrogen functional genes
Land use change
Jiulong River

ABSTRACT

Human activities have largely modified nitrogen (N) sources supply, cycling and export from land to ocean. Nitrification and denitrification are vital processes alleviating N pollution in aquatic ecosystems but the diverse responses and niche of microbial N retention to human disturbance are still understudied. Here we investigated the changes in N species and functional genes in the urban, agriculture and reservoir river sections of the Jiulong River (southeast China). Our results show that ammonia-oxidizing bacteria (AOB) (*Nitrosomonas*) were dominant in the urban river section receiving ammonium-rich sewage that enhanced nitrification and subsequent denitrification, while ammonia-oxidizing archaea (AOA) was more abundant than AOB in the river section flowing through areas of pomelo (*Citrus maxima*) agriculture with low pH, low ammonium and very high nitrate input. Warm temperatures and large total suspended matter (TSM) in the wet season promoted growth of nitrifiers and denitrifiers, which were mostly particle-attached. The potential river N retention through gaseous N removal (PR_{N2O} and PR_{N2}) in the agriculture section with huge N loading was among the lowest. Strong nitrification and denitrification were suspected to occur in the agricultural acid soil system rather than in the river network. In addition, the decreased TSM and N concentration promoted free-living microbes in the reservoir. The highest PR_{N2} and N_2 production observed in the reservoir in the dry season implied that denitrification and anammox occurring in sediments was likely to increase N retention. This study suggests the diverse factors involved in processing of N pollution among diverse landscapes.

* Corresponding author at: College of the Environment and Ecology, Xiamen University, Xiamen 361102, China.
E-mail address: nwchen@xmu.edu.cn (N. Chen).

https://doi.org/10.1016/j.scitotenv.2020.141139
0048-9697/

1. Introduction

Land use change and increased loading of anthropogenic nitrogen (N) to earth systems have resulted in eutrophication, harmful algal blooms, hypoxia and biodiversity reduction (Galloway et al., 2004; Hagy et al., 2004; Maloney and Weller, 2011). A coupled nutrient input–hydrology–instream nutrient retention model (IMAGE-GNM) suggest that human activities have led to a global increase in river nutrient transport to the ocean during the 20th century despite increased retention along the aquatic continuum (Beusen et al., 2016). Nitrogen retention in the aquatic continuum includes temporary storage in plant biomass, trapping of sediment and particulate, permanent loss via gaseous N removal by nitrification-denitrification, exchange between sediment and water column, and so on (Bouwman et al., 2013). In recent decades, major rivers discharging along the east coast of China have been considered to be hot spots of regional N pollution due to chemical fertilizer consumption, urbanization, river damming and aquaculture (Lin et al., 2020; Yu et al., 2019a). Understanding N biogeochemical processes and response to human disturbance in river networks is of great importance in order to successfully manage nutrient pollution and restore aquatic ecosystems.

Nitrification and denitrification are two vital biogeochemical processes regulating aquatic ecosystem functioning and ability to supply services to human society. Nitrification is a two-step biological oxidization process, conducted by ammonia-oxidizing and nitrite-oxidizing autotrophic microbes, from NH_4^+-N to NO_2^--N and NO_3^--N (Daims et al., 2016). Traditional denitrification (i.e. heterotrophically anaerobic denitrification) involves the reduction of NO_3^--N, via NO_2^--N and NO, to N_2O and N_2 (Akunna et al., 1992). Coupled nitrification-denitrification enhances N retention in redox-variable conditions, such as suspended sediments, bed-sediments and aquatic environments (Xia et al., 2017). After *T. pantotropha* was found to be an aerobic denitrifier in 1984 (Dalsgaard et al., 2003; Kuypers et al., 2003), Yang et al. (2020) clarified the mechanism of aerobic denitrification from the perspective of electron transfer. Anammox also produce N_2, which has been widely known to occur in anaerobic conditions (Strous et al., 1997). Although these processes are widespread and important to transform and remove N, the diverse responses of nitrification and denitrification to human disturbance are understudied.

Environmental biologists have often reported the abundance and community of nitrifiers and denitrifiers from various river waters and sediments (Huang et al., 2011; Liao et al., 2018; Lin et al., 2020; Liu et al., 2011; Lv et al., 2017; Zhou et al., 2015). Damashek et al. (2015) found that the abundance and community of ammonia-oxidizing bacteria (AOB) and archaea (AOA) were different in water and sediment samples that were influenced by agricultural runoff and sewage effluent, and both were found to be more abundant in agricultural sediments than in residential and industrial areas (Zhang et al., 2016). The community of archaea (e.g. AOA) in the Jiulong River was found to be sensitive to water temperature, nutrient concentrations and stoichiometry (Hu et al., 2016). Johnson et al. (2012) found that the composition of denitrifying communities were little affected by local sediment organic carbon in an agricultural stream, but other literature reported that denitrification rates increased with DOC (Arango et al., 2007; Inwood et al., 2007). Such heterogeneity of nitrifier and denitrifier genes might be explained by variety in habitat type and environmental conditions. Geochemists have extensively measured concentration and composition of N species at various temporal and spatial scales, but their results typically lack biological interpretation. Therefore, an interdisciplinary research linking nitrifier and denitrifier genes and physicochemistry is essential to better understand the impacts of human disturbance on the biogeochemical N cycle.

The development of urbanization, agriculture and dam reservoir construction have been identified as major contributors to changes the N budget, riverine N cycling and export in the Jiulong River watershed (Chen et al., 2014a; Chen et al., 2008; Chen et al., 2015; Chen et al., 2014b; Gao et al., 2018; Yu et al., 2015). The further question we seek to address here is how these human disturbances impact microbial nitrification and denitrification. In this study we investigated the changes in N species, functional genes (*amo*A (AOA), *amo*A (AOB), *nxr*A, *nar*G, *nir*S, *hzs*B) and 16S rRNA between urban, agriculture and reservoir sections of the Jiulong River (southeast China) during the wet and dry season in 2018. Specific objectives of the study were to: (1) clarify anthropogenic N inputs that influence nitrification and denitrification in river sections; (2) reveal hydroclimatic controls on the different nitrifiers and denitrifiers and therefore on differences in gaseous N retention between the urban and agriculture river sections; and (3) examine major factors controlling reservoir nitrification and denitrification and associated N retention.

2. Materials and methods

2.1. Study area

The Jiulong River (JR) is located on the western coast of the Taiwan Strait and is the second largest river in Fujian province (Fig. 1, Table S1), with a catchment area of 14,741 km^2. Two main tributaries combined totally export 12.4×10^9 m^3 y^{-1} freshwater to the Jiulong Estuary; the North Jiulong River (NJR) exports about two-thirds of this discharge while the West Jiulong River (WJR) exports one-third (Yu et al., 2019b). The topography of the NJR drainage area is hillier than the WJR (Gao et al., 2018). The multi-year average rainfall in the watershed is 1400–1800 mm, and 62% of precipitation occurred in the wet season (May to September in 2018).

This study targeted three river sections which are mainly influenced by urban sewage discharge, orchard agricultural runoff and cascade-dam construction, respectively. The urban river section in the upper NJR passes through the city of Longyan and several other towns. In 2018, the human population of Longyan was 0.74 million, and the number of pigs feeding was 0.98 million. The agriculture river section in the upper WJR (Pinghe county) was dominated by pomelo (*Citrus maxima*) planting in catchment. The reservoir section in the lower NJR was mainly regulated by cascade hydropower reservoirs (Zhou et al., 2016). More details about the JR watershed have been described in Chen et al. (2014b).

2.2. Sampling campaign

We conducted two samplings in July (wet season) and November (dry season) 2018 (Fig. S1). Sampling was targeted at four urban river sites (U1-U4), four agriculture river sites (A1-A4) and four reservoir sites (R1-R4) (Fig. 1). Based on results obtained in the wet season, it was necessary to sample additional tributary sites in the urban river section (U1-1 and U1-2) and agriculture river section (A2-1 and A3-1). Surface (0.5 m) water was collected by a 5 L plexiglass sampler for analysis of nutrient forms and microbes. In the dry season, additional water samples for dissolved gases analysis were introduced into 12 mL Labco bottles (N_2) and 60 mL brown glass bottles (N_2O) using a silicone tube until overflow of about 3+ volumes of water. The bottles were immediately capped without air space after adding a final concentration of 0.1% $HgCl_2$ to stop microbial activity. All samples were stored in a cooler at 4 °C and immediately delivered to the lab for filtration and analysis. Dissolved oxygen (DO), water temperature and pH were measured in-situ using a WTW multi-parameter portable meter (Multi 3430, Germany).

2.3. Physicochemical analysis

About 300 mL of water samples were filtered by a GF/F membrane for nutrient analysis and determination of total suspended matter (TSM). TSM weight was calculated by the differences between the unfiltered and filtered GF/F membranes after oven-drying (105 °C) to constant weights. Ammonium (NH_4^+-N), nitrite (NO_3^--N) and

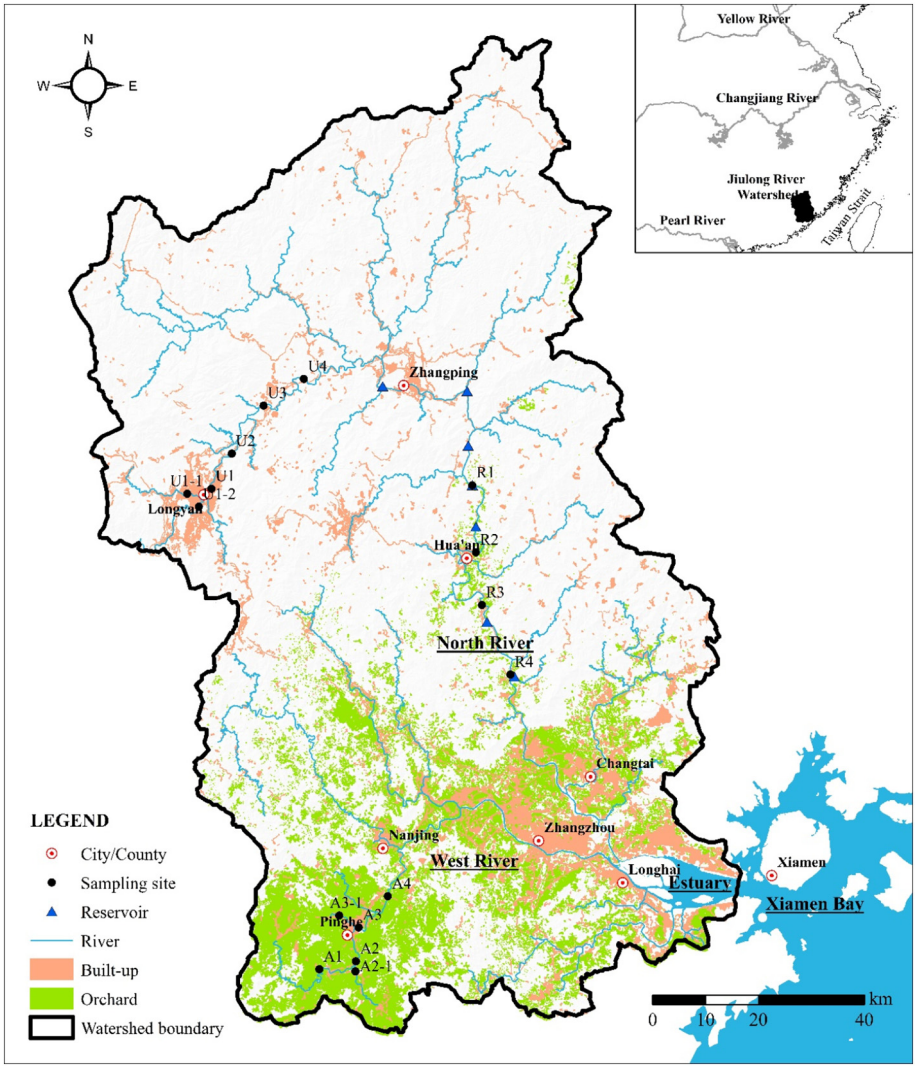

Fig. 1. Map of the Jiulong River watershed showing study sites. Three river sections (urban, agriculture and reservoir) were selected for the comparative study and named U, A and R, respectively.

nitrate (NO_2^--N) of filtrate was detected by segmented flow automated colorimetry (San++ analyzer, Germany). Dissolved inorganic N (DIN) was the sum of NH_4^+-N, NO_3^--N and NO_2^--N. Dissolved total N (DTN) was determined as NO_3^--N following oxidization with 4% alkaline potassium persulfate. Dissolved organic N (DON) was calculated by subtracting DIN from DTN. The precision of the N components was determined by repeated 10% samples, and the relative error was less than 5%.

Concentration of dissolved N_2 was measured using membrane inlet mass spectrometry (MIMS) and the N_2:Ar ratio method (Chen et al., 2014b). Concentration of dissolved N_2O was measured by Gas Chromatograph (GC) (Agilent 7890A, US). Excess dissolved N_2 (ΔN_2) was calculated using Eq. (1), where ΔN_2 is a measure of net N_2 production (gross denitrification minus gross N fixation). Excess dissolved N_2O (ΔN_2O) was calculated using Eq. (2). ΔN_2 and ΔN_2O indicate net production of gaseous N from sediments and water column.

$$\Delta N_2 = [N_2 : Ar]_{measured} \times [Ar]_{expected} - [N_2]_{expected} \quad (1)$$

where $[N_2{:}Ar]_{measured}$ is the detected N_2:Ar ratio by MIMS; $[Ar]_{expected}$ and $[N_2]_{expected}$ were calculated by Weiss equations based on sampling temperature and salinity (Weiss, 1970).

$$\Delta N_2O = [N_2O]_{measured} - [N_2O]_{expected} \quad (2)$$

where $[N_2O]_{measured}$ is the measured concentration in surface water by GC; $[N_2O]_{expected}$ is calculated by Weiss equations (Weiss and Price, 1980), and the atmospheric N_2O concentration is taken from http://www.cmdl.noaa.gov/.

2.4. Molecular analysis

Aquatic microbes can be classified as free-living (FL) or particle-attached (PA) (Crump et al., 1999). About 1 L of water samples for analysis of N functional gene abundance were filtered by a 20 μm bluteau before sequential filtration by a 3 μm and 0.22 μm Isopore TM Membrane (47 mm, Millipore, USA). The 0.22 and 3 μm filters respectively collected FL and PA microbes. All filters were stored in a −80 °C freezer until DNA extraction.

DNA extraction from filters was performed by FastDNA™ Spin Kit for Soil (Millipore, USA), suspended in 80 μL TE solution and stored at −80 °C until analysis. Concentration and purity of the DNA was quantified by a Nano Drop spectrophotometer (DN-1000; Isogen Life Science, the Netherlands). The maximum abundant denitrifying genes of first step (*nap*A and *nar*G) and the second step (*nir*K and *nir*S) were selected by a high-throughput qPCR-based functional-gene chip detection method (QMEC) (Fig. S2) (Zheng et al., 2018). Primer pairs, cycle thresholds, amplification protocols, regression functions, amplification efficiencies and limit of detection of nitrifier genes (*amo*A (AOA),

*amo*A (AOB) and *nxr*A), denitrifier genes (*nar*G and *nir*S), anammox gene (*hzs*B) and 16S rRNA in absolute qPCR (Bio-Rad) were shown in Tables S2, S3, S4 and S5, respectively. For these genes, the abundances were quantified by a Bio-Rad CFX96 qPCR in triplicate with three negative controls (no DNA template) and five standards. Each sample received 10 μL of Hieff™ SYBR Master Mix (Yeasen, China), 0.4 × 2 μL of primers (10 μmol L^{-1}), 1 μL of template DNA and 8.2 μL of double distilled H_2O. The ratios of functional gene abundance to 16S rRNA abundance indicated the relative abundance (RA). Absolute gene abundance indicated the AA.

AOA and AOB was sequence on an Illumina MiSeq instrument using 2 × 300 bp lengths with 40–50 K reads by the company GENEWIZ (China). The sequencing primers of AOA and AOB were the same as qPCR. High-throughput sequence processing was conducted by Mothur software v.1.35.1 (Schloss et al., 2009). Quality-controlled sequences were obtained after removal of tags and primers. All samples were analyzed at the same sequencing depth (10000) after the *sub.sample* command. Sequences were simplified using the *unique.seqs* command and then aligned to newly developed database of *amo*A gene using the *align.seqs* command. Badly aligned sequences were filtered using the *screen.seqs* command. In order to improve sequencing quality, the *pre.cluster*, *chimera.uchime* and *remove.seqs* commands were used. After removing barcode sequences, binning, denoising, and trimming sequences, the quality-trimmed sequences were aligned to *amo*A (AOA or AOB) gene databases from GenBank (https://www.ncbi.nlm.nih.gov/genbank/) and FunGene (http://fungene.cme.msu.edu/) (He et al., 2018; Yang et al., 2014). Following the *classify.seqs* command, each operational taxonomic unit (OTU) was defined by 89.4% sequence identity for diversity analyses (He et al., 2018). The "*unknown*" sequences were removed by the *remove.lineage* command. Rarefaction, non-parametric coverage, Chao 1, Shannon and Simpson were calculated with commands of *dist.seqs*, *cluster, make.shared*, *classify.otu*, *rarefaction.single*, *remove.rare* and *summary.single*. The raw Illumina reads of *amo*A gene sequences were deposited in the NCBI archive under the accession of No. PRJNA630008 (AOA) and No. PRJNA630007 (AOB).

2.5. Auxiliary data and statistical analysis

The antecedent precipitation index (API) can be used to indicate the soil antecedent moisture condition (Perrone and Madramootoo, 1998). API in the three river sections (urban, agriculture and reservoir) was calculated according to Eq. (3), based on precipitation recorded by nearby meteorological stations (Longyan, Pinghe and Hua'an). According to the API value, soil condition was classified as dry (0 ≤ API ≤ 15 mm), average (15 < API ≤ 30 mm) and wet (API > 30 mm).

$$\mathrm{API} = \sum_{i=0}^{n} P_i \times K^i \tag{3}$$

where P_i is the amount of precipitation 1,2,…,i ($i = 14$) days prior to the event, and $K = 0.85$ is the recession coefficient.

The potential retention of N_2O (PR_{N2O}) and N_2 (PR_{N2}) defined by Eqs. (4) and (5) indicates the strength of gaseous N retention in the river system. We assumed that N_2O was produced from NH_4^+-N by nitrification and NO_3^--N by denitrification. N_2 was mainly produced by denitrification of NO_3^--N.

$$\mathrm{PR_{N2O}} = [\Delta N_2O]/([NH_4{}^+ - N] + [NO_3{}^- - N]) \tag{4}$$

$$\mathrm{PR_{N2}} = [\Delta N_2]/[NO_3{}^+ - N] \tag{5}$$

Redundancy analysis (RDA) was performed using Canoco 5. The select analysis type of clustered samples was performed using the command of *constrained ordination of species, with selection of environmental variables*. The significant environmental variables were determined by p-value < 0.05. Summary of redundancy analysis and statistical significance of environmental variables were shown in Tables S6 and S7, respectively. R 3.5.1 was used for correlation analysis between the N functional genes and environmental variables. SPSS 19.0 were used to perform ANOVA analysis to test between-groups and within-groups difference among river sections following the Kolmogorov-Smirnov test and variances homogeneous test.

Table 1
Absolute gene abundances and the ratios of absolute gene abundance to 16S rRNA abundance in the urban, agriculture and reservoir river sections.

Gene			Wet season			Dry season		
			Urban	Agriculture	Reservoir	Urban	Agriculture	Reservoir
Nitrifier	*amo*A (AOA)	AA	$1.1 \times 10^3 \pm 0.9 \times 10^3$	$1.1 \times 10^3 \pm 0.8 \times 10^3$	$0.9 \times 10^3 \pm 1.0 \times 10^3$	$0.7 \times 10^3 \pm 0.3 \times 10^3$ b	$6.8 \times 10^3 \pm 5.6 \times 10^3$ a	$0.1 \times 10^3 \pm 0.1 \times 10^3$ c
		RA	$5.6 \times 10^{-7} \pm 6.1 \times 10^{-7}$	$2.5 \times 10^{-7} \pm 3.8 \times 10^{-7}$	$5.4 \times 10^{-7} \pm 7.1 \times 10^{-7}$	$0.2 \times 10^{-7} \pm 0.1 \times 10^{-7}$ b	$1.9 \times 10^{-7} \pm 2.0 \times 10^{-7}$ a	$0.1 \times 10^{-7} \pm 0.03 \times 10^{-7}$ b
	*amo*A (AOB)	AA	$0.5 \times 10^3 \pm 0.1 \times 10^3$	$0.3 \times 10^3 \pm 0.2 \times 10^3$	$1.4 \times 10^3 \pm 1.5 \times 10^3$	$0.7 \times 10^3 \pm 0.2 \times 10^3$ a	$0.5 \times 10^3 \pm 0.3 \times 10^3$ a	$0.1 \times 10^3 \pm 0.1 \times 10^3$ b
		RA	$2.1 \times 10^{-7} \pm 1.2 \times 10^{-7}$	$0.5 \times 10^{-7} \pm 0.5 \times 10^{-7}$	$8.9 \times 10^{-7} \pm 9.9 \times 10^{-7}$	$2.1 \times 10^{-8} \pm 1.4 \times 10^{-8}$	$1.2 \times 10^{-8} \pm 0.6 \times 10^{-8}$	$0.6 \times 10^{-8} \pm 0.4 \times 10^{-8}$
	*nxr*A	AA	$0.3 \times 10^3 \pm 0.2 \times 10^3$ b	$3.3 \times 10^3 \pm 3.3 \times 10^3$ a	$0.3 \times 10^3 \pm 0.3 \times 10^3$ b	$0.3 \times 10^3 \pm 0.1 \times 10^3$ b	$0.5 \times 10^3 \pm 0.3 \times 10^3$ a	$0.1 \times 10^3 \pm 0.1 \times 10^3$ b
		RA	$1.0 \times 10^{-7} \pm 0.2 \times 10^{-7}$ b	$2.8 \times 10^{-7} \pm 1.5 \times 10^{-7}$ a	$1.2 \times 10^{-7} \pm 0.3 \times 10^{-7}$ b	$5.2 \times 10^{-9} \pm 3.3 \times 10^{-9}$ b	$9.8 \times 10^{-9} \pm 2.8 \times 10^{-9}$ a	$5.2 \times 10^{-9} \pm 0.6 \times 10^{-9}$ b
Denitrifier	*nar*G	AA	$1.7 \times 10^5 \pm 2.3 \times 10^5$ a	$0.6 \times 10^5 \pm 0.4 \times 10^5$ b	$0.2 \times 10^5 \pm 0.2 \times 10^5$ b	$1.0 \times 10^5 \pm 0.8 \times 10^5$ a	$0.2 \times 10^5 \pm 0.1 \times 10^5$ b	$0.04 \times 10^5 \pm 0.02 \times 10^5$ c
		RA	$5.1 \times 10^{-5} \pm 5.2 \times 10^{-5}$ a	$0.4 \times 10^{-5} \pm 0.4 \times 10^{-5}$ b	$0.6 \times 10^{-5} \pm 0.2 \times 10^{-5}$ b	$2.8 \times 10^{-6} \pm 2.7 \times 10^{-6}$ a	$0.6 \times 10^{-6} \pm 0.3 \times 10^{-6}$ b	$0.3 \times 10^{-6} \pm 0.1 \times 10^{-6}$ b
	*nir*S	AA	$1.7 \times 10^5 \pm 0.4 \times 10^5$	$1.6 \times 10^5 \pm 0.8 \times 10^5$	$1.4 \times 10^5 \pm 0.7 \times 10^5$	$0.5 \times 10^5 \pm 0.3 \times 10^5$ a	$0.4 \times 10^5 \pm 0.2 \times 10^5$ a	$0.1 \times 10^5 \pm 0.1 \times 10^5$ b
		RA	$0.9 \times 10^{-6} \pm 0.3 \times 10^{-6}$	$3.0 \times 10^{-6} \pm 1.5 \times 10^{-6}$	$1.0 \times 10^{-6} \pm 0.8 \times 10^{-6}$	$1.4 \times 10^{-6} \pm 0.9 \times 10^{-6}$ a	$0.9 \times 10^{-6} \pm 0.3 \times 10^{-6}$ a	$0.5 \times 10^{-6} \pm 0.2 \times 10^{-6}$ b
Anammox	*hzs*B	AA	$1.4 \times 10^3 \pm 0.9 \times 10^3$	$1.9 \times 10^3 \pm 0.8 \times 10^3$	$2.7 \times 10^3 \pm 2.3 \times 10^3$	$0.2 \times 10^4 \pm 0.5 \times 10^4$	$1.2 \times 10^4 \pm 1.8 \times 10^4$	$0.3 \times 10^4 \pm 0.3 \times 10^4$
		RA	$0.6 \times 10^{-6} \pm 0.5 \times 10^{-6}$	$0.2 \times 10^{-6} \pm 0.2 \times 10^{-6}$	$1.1 \times 10^{-6} \pm 1.0 \times 10^{-6}$	$0.9 \times 10^{-7} \pm 2.1 \times 10^{-7}$	$5.1 \times 10^{-7} \pm 8.9 \times 10^{-7}$	$1.2 \times 10^{-7} \pm 1.4 \times 10^{-7}$
16S rRNA		AA	$0.3 \times 10^{10} \pm 0.1 \times 10^{10}$	$1.3 \times 10^{10} \pm 1.2 \times 10^{10}$	$0.4 \times 10^{10} \pm 3.3 \times 10^{10}$	$6.6 \times 10^{10} \pm 7.4 \times 10^{10}$ a	$5.1 \times 10^{10} \pm 2.8 \times 10^{10}$ a	$1.6 \times 10^{10} \pm 1.2 \times 10^{10}$ b

Note: data are presented as mean ± standard deviation in unit of copies mL^{-1}. a, b, c represent significant differences ($p < 0.05$) among the river sections of urban (U), agriculture (A) and reservoir (R). Absolute abundances (AA) (copies mL^{-1}) are the numbers calculated by qPCR. Relative abundances (RA) are the ratio of functional gene abundances to 16S rRNA. Site U3 is outlier for absolute abundance, where can be affected by the tributary Gaojuxi River. ANOVA tests were confirmed by Kolmogorov-Smirnov test and Normality plots with t-test. All data are total numbers including free-living and particle-attached abundance. The absolute free-living and particle-attached abundance for each samples are displayed in Table S8.

Additional physico-chemical parameters and gaseous N measured in 2011 (Chen et al., 2015; Chen et al., 2014b) were integrated into the analysis to improve understanding of the temporal and spatial variation of nitrification and denitrification in the study river.

3. Results

3.1. Spatial and temporal variation of gene abundances

The qPCR-based analysis of *amo*A (AOA), *amo*A (AOB), *nxr*A, *nar*G, *nirS*, *hzs*B and 16S rRNA genes successfully captured the variation between river sections and seasons. The average total AA of these genes ranged from 14 to 1.7×10^4 (AOA), 15 to 3.7×10^3 (AOB), 22 to 7.1×10^3 (*nxr*A), 1.1×10^3 to 5.0×10^5 (*nar*G), $2.8 \times 10^3$to 2.1×10^5 (*nir*S), 25 to 4.6×10^4 (*hzs*B) and 1.3×10^9 to 2.0×10^{11} (16S rRNA) copies per milliliter (Table 1).

There were different gene abundances between agriculture, urban and reservoir river sections. AOA had higher AA and RA in the agriculture river section (Table 1), where AOA increased but AOB changed little resulting in higher ratio of AOA/AOB (Fig. 2a). The abundance of nitrifying gene *nxr*A was less than *amo*A (Fig. 2b), and *nxr*A was relatively higher in the agriculture river section ($p < 0.05$) (Table 1). The denitrifier gene *nar*G was more abundant than nitrifier gene *nxr*A, and the maximum ratio of *nar*G/*nxr*A (Fig. 2c) and the maximum RA of *nar*G were found in the urban river section (Table 1). The ratio *nar*G/*nir*S was less than one in the agriculture river section, but it was greater than one in the urban river section (Fig. 2d). Average AA and RA of *hzs*B were lower in the urban river section. AA of all genes in the reservoir section were the lowest (Table 1).

Most genes had a higher AA and RA in the wet season than in the dry season with the exceptions of the agriculture river sites, where *amo*A (AOA) was higher in the dry season (Table 1). In the wet season, more *nxr*A (3.3×10^3 copies mL^{-1}) was observed in the agriculture river section ($p < 0.05$), but more RA of *amo*A (AOB) (2.1×10^{-7}) and more AA and RA of *nar*G (1.7×10^5 copies mL^{-1} and 5.1×10^{-5}) were detected in the urban river section. In the dry season, the agriculture river section had a higher AA and RA of *amo*A (AOA) (6.8×10^3 copies mL^{-1} and 1.9×10^{-7}) and *nxr*A (5.0×10^2 copies mL^{-1} and 9.8×10^{-9}) ($p < 0.05$), while the urban river section had a higher AA and RA of *nar*G (1.0×10^5 copies mL^{-1} and 2.8×10^{-6}) ($p < 0.05$). In the reservoir, all genes except *hsz*B had more AA and RA in the wet season than in the dry season (Table 1).

The majority of genes were particle-attached (PA) in the urban ($79 \pm 14\%$) and agriculture river sections ($83 \pm 12\%$), but *nar*G and *hzs*B genes were mainly present as free-living (FL) microbes in the urban and agriculture river sections (Fig. 3, Table S8). The reservoir had relatively more free-living *amo*A (AOA $64 \pm 29\%$, AOB $44 \pm 9\%$), *nar*G (99%), *nir*S ($36 \pm 9\%$) and 16S rRNA ($33 \pm 14\%$) than other sections, except *hzs*B with $93 \pm 13\%$ was PA (Fig. 3).

3.2. Diversity of ammonia-oxidizing microbial communities

Diversity of archaeal and bacteria *amo*A genes were compared in river water, sediments and bank slope soil of the agriculture and urban river section in the dry season (2018). The gentle rarefaction curves can certify the sufficient amount of sequence to analyze AOA and AOB diversity (Fig. 4c,d). Both AOA and AOB, higher diversity (high Shannon, high Chao 1, high Ace, more OTUs and low Simpson)

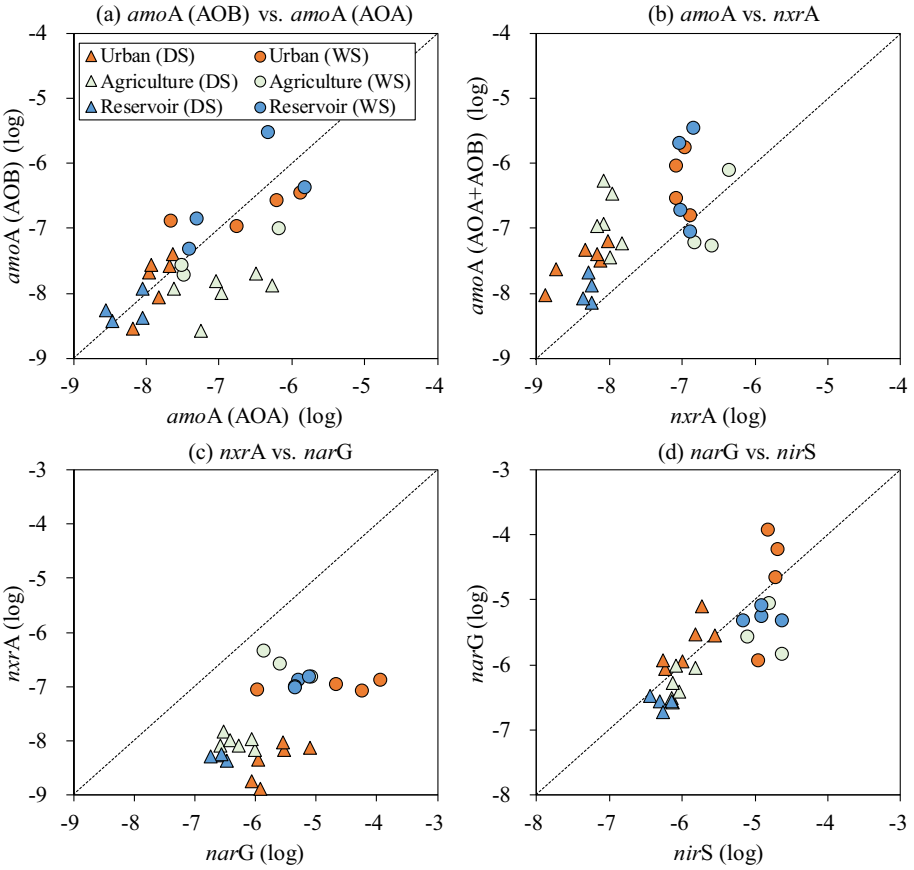

Fig. 2. Relative abundance of *amo*A (AOA and AOB), *nxr*A, *nar*G and *nir*S gene abundances in 2018. DS: dry season; WS: wet season.

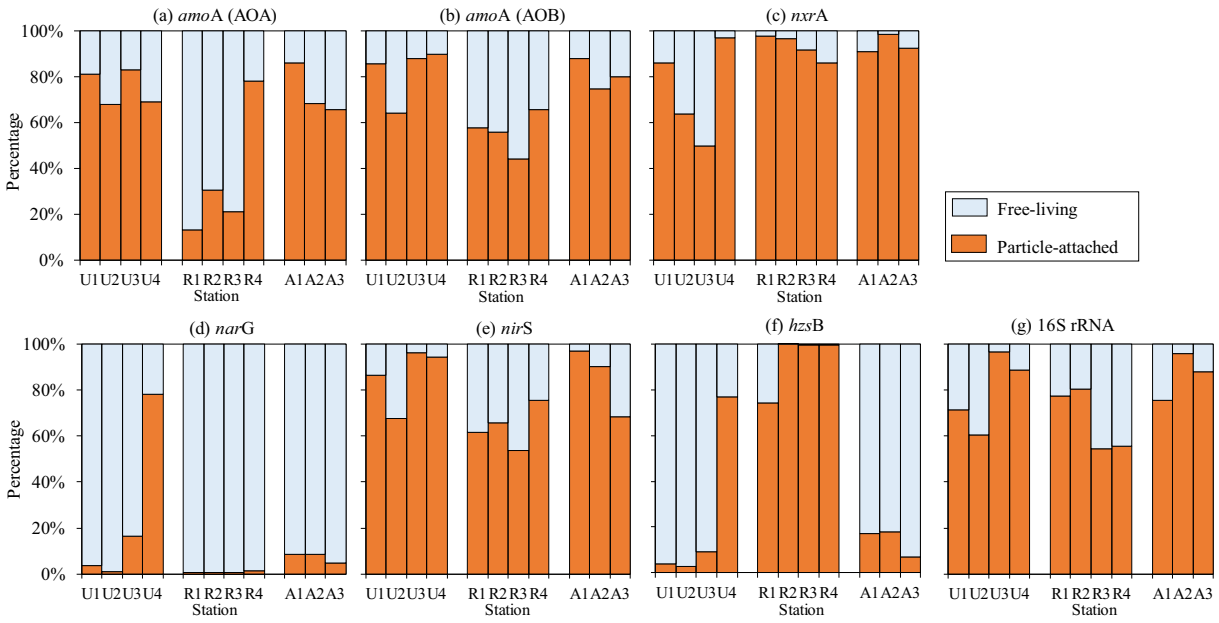

Fig. 3. The percentage of free-living and particle-attached gene abundance in the wet season (July-2018).

was found in river water, but lower diversity was in bank slope soil samples (Table 2). Higher diversity of AOA and AOB was detected in the agriculture river section (Table 2).

AOA in the agriculture and urban river section was clustered to Group I.1a (*Nitrosotenuis*, *Nitrosopumilus*, *Nitrosoarchaeum* and *Nitrosopelagicus*), Group I.1a-associated (*Nitrosotalea*) and Group I.1b (*Nitrososphaera*) (Fig. 4a). Soil cluster (*Nitrososphaera*) had higher relative abundance in sediment and river slope soil, which was the maximum cluster of soil samples especially in the agriculture river section. Acidophilic cluster (*Nitrosotalea*) was up to 13.7% in water at the closet site to

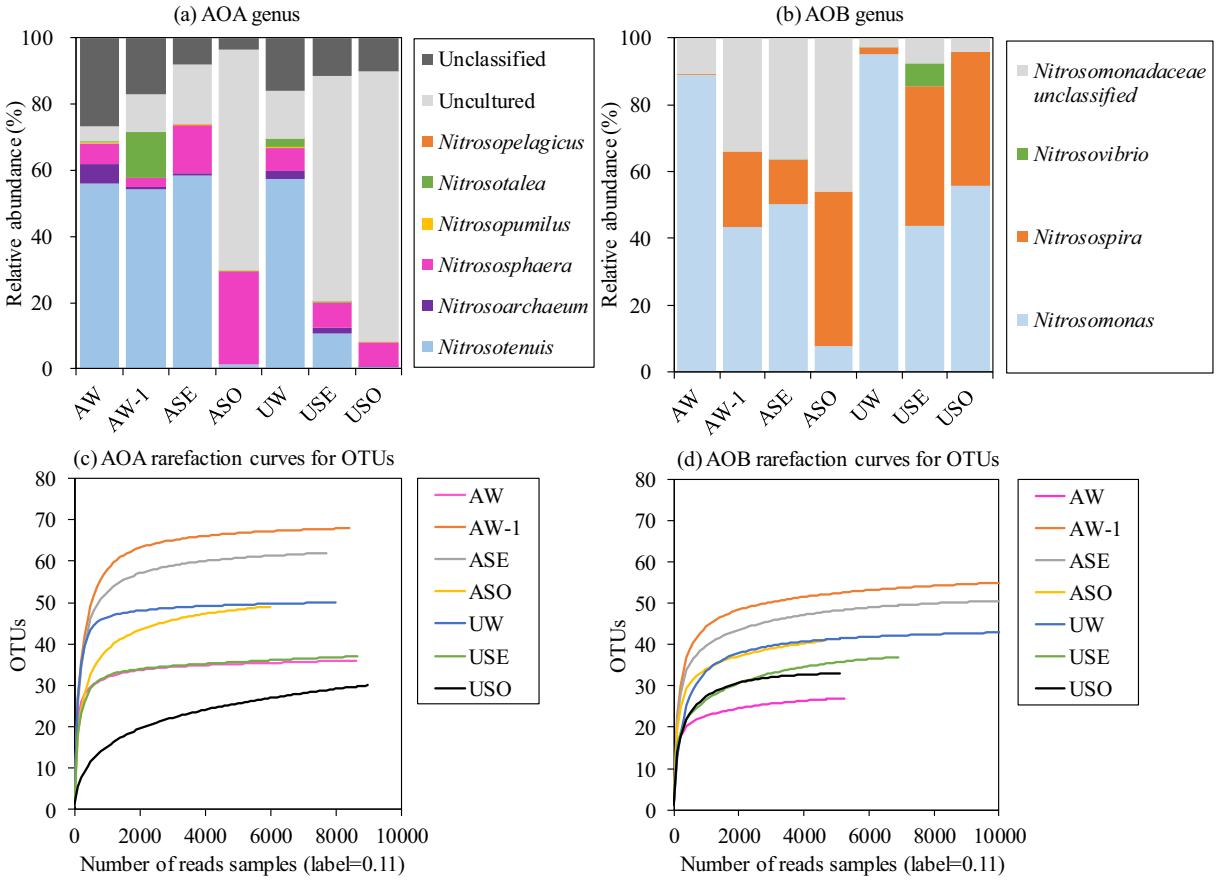

Fig. 4. Relative abundance and rarefaction curves (OTUs) of AOA and AOB at genus level between agriculture (A) and urban (U) in the dry season (2018). AW is the mixed water samples of sites A2, A3 and A4. AW-1 is the water sample of site A3-1. ASE is the mixed sediment samples of sites A1 and A2. ASO is the mixed soil samples of sites A1 and A2. UW is the mixed water sample of sites U1, U2, U3 and U4. USE is the mixed sediment samples of sites U2 and U3. USO is the mixed soil samples of sites U2 and U3.

Table 2
The alpha diversity index of water, sediment and soil samples in the urban and agriculture river sections.

Gene	Sample	Initial reads	High-quality reads	Coverage	Simpson	Chao1	Shannon	Ace	OTUs
*amo*A (AOA)	AW	25,115	9061	100%	0.11	35.90	2.69	36.00	36
	AW-1	26,126	9057	100%	0.12	68.36	2.87	68.19	68
	ASE	37,171	8180	100%	0.18	62.90	2.59	62.62	62
	ASO	22,081	6047	100%	0.38	50.50	1.83	51.15	49
	UW	35,678	8696	100%	0.10	50.00	2.91	50.51	50
	USE	37,397	9183	100%	0.35	39.17	1.90	42.75	37
	USO	67,854	9504	100%	0.79	36.67	0.55	38.02	30
*amo*A (AOB)	AW	69,231	5719	100%	0.11	27.49	2.46	29.07	27
	AW-1	56,906	8073	100%	0.14	55.26	2.60	54.71	56
	ASE	50,936	8462	100%	0.14	50.99	2.60	52.38	51
	ASO	63,456	5576	100%	0.11	42.50	2.62	44.84	41
	UW	86,952	8656	100%	0.50	42.58	1.35	42.48	43
	USE	62,265	7690	100%	0.12	38.45	2.43	39.97	37
	USO	50,294	6170	100%	0.23	33.07	1.99	33.25	33

Note: AW is the mixed water samples of sites A2, A3 and A4. AW-1 is the water sample of site A3-1. ASE is the mixed sediment samples of sites A1 and A2. ASO is the mixed soil samples of sites A1 and A2. UW is the mixed water sample of sites U1, U2, U3 and U4. USE is the mixed sediment samples of sites U2 and U3. USO is the mixed soil samples of sites U2 and U3. Sampling sites refer to Fig. 1.

the orchard. *Nitrosotenuis* was the maximum cluster in water and sediment samples.

AOB mostly came from *Nitrosomonas* and *Nitrosospira* (Fig. 4b). The maximum relative abundance of *Nitrosomonas* was up to 95.3% in water in the urban river section (UW). The maximum relative abundance of *Nitrosospira* was up to 46.6% in river bank slope soil samples from the agriculture river section and up to 22.9% in river water next to the orchard.

3.3. Hydrological and physicochemical characteristics

The hydrological conditions changed with seasons. Average water temperature increased from 23.3 °C in the dry season (November) to 31.7 °C in the wet season (July) (Table S1). API of sampling sites ranged from 4 to 39 mm with the largest variation in the agriculture river section (Table S1). A high API in the wet season corresponded to higher N concentrations and PR_{N2O} and PR_{N2} (Tables 3, S9).

Physicochemical characteristics varied across river sections. TSM was highest in the urban river section, followed by the agriculture river and the reservoir section. 73.2% to 79.1% surface sediments were bigger than 3.9 μm, but the maximum percentage (26.8% ± 9%) of fine particle (size < 3.9 μm) was found in the reservoir section (Table S10). Nitrogen concentrations also exhibited a clear spatial variation (Fig. 5, Table S9). Higher NH_4^+-N and NO_2^--N were observed in the urban river section, but higher NO_3^--N, DIN and DON were detected in the agriculture river section. Nitrogen concentrations were lowest in the reservoir sites. PR_{N2O} and PR_{N2} were higher in the urban river section than in the agriculture sites (Fig. 5, Table S9). PR_{N2} in the reservoir was highest in the dry season, while PR_{N2O} was among the lowest. Low DO (6.0 ± 1.0 mg L^{-1}) and high pH (7.4 ± 0.2) in the urban river section mostly were significantly different ($p < 0.05$) from the agriculture river section which had high DO (7.7 ± 1.8 mg L^{-1}) and low pH (7.2 ± 0.4) (Table S9).

Averaged concentrations of NH_4^+-N and NO_3^--N in the dry season were higher than in the wet season (Fig. 5). In contrast, NO_2^--N, as an intermediate product of nitrification and denitrification, was higher in the wet season (17.3 ± 11.8 μmol L^{-1}) compared to the dry season (11.4 ± 8.4 μmol L^{-1}), with a significant seasonal difference in the urban river section (2011) ($p = 0.03$) and reservoir (2018) ($p = 0.03$) (Fig. 4b). PR_{N2O} and PR_{N2} were higher in the wet season and the period of API > 30 in the urban and agriculture river sections (Fig. 5, Table 3). In the reservoir, PR_{N2} was higher in the dry season (October 2011 and November 2018) than the wet season (May 2011) along the river network. In the agriculture river section (2018), pH was lower in the dry season (7.03 ± 0.3) than in the wet season (7.54 ± 0.7), while TSM was higher in the dry season (10.84 ± 2.16 mg L^{-1}) than in the wet season (8.26 ± 2.63 mg L^{-1}) (Table S9).

3.4. Relationship between nitrogen functional genes and environmental factors

RDA was performed to explore the main environmental factors influencing N functional genes in the urban and agriculture river sections in the wet and dry seasons (Fig. 6). NO_3^--N, DON and DO could be the major factors affecting nitrifiers and denitrifiers in the agriculture river section. pH had a negative relationship with *amo*A (AOA) in the dry season in the agriculture river section. NH_4^+-N, NO_2^--N and TSM were the main controlling factors in the urban river section, which had a positive correlation with each other (Fig. S3).

The strength of N-gene relationship changed with season. In the wet season, NO_3^--N, NH_4^+-N, DIN and TSM had a significant correlation with

Table 3
Gaseous N removal (ΔN_2 and ΔN_2O) and potential retention (PR_{N2} and PR_{N2O}) in three river sections.

Land use	Date	API	ΔN_2O (nmol L^{-1})	ΔN_2 (μmol L^{-1})	PR_{N2O} (%)	PR_{N2} (%)
Urban	Nov-2018	≤30	21.3 ± 4.0[b]	9.1 ± 9.8[b]	0.01 ± 0.002[b]	6.2 ± 6.6[b]
	May-2011, Oct-2011	>30	62.7 ± 14.5[a]	35.4 ± 10.1[a]	0.014 ± 0.002[a]	14.6 ± 7.4[a]
Agriculture	Oct-2011, Nov-2018	≤30	41.6 ± 17.6	17.4 ± 13.3	0.005 ± 0.002	2.9 ± 2.8
	May-2011	>30	28.7 ± 1.6	53.3 ± 20.9	0.008 ± 0.003	4.5 ± 0.8
Reservoir	May-2011, Nov-2018	≤30	16.2 ± 14.7	13.2 ± 8.1	0.005 ± 0.003	8.4 ± 3.8
	Oct-2011	>30	10.9 ± 5.4	52.3 ± 26.7	0.004 ± 0.002	25.3 ± 13.5

Note: data for 2011 were adapted from previous studies (Chen et al., 2015; Chen et al., 2014b). The antecedent precipitation index (API) reflects the soil antecedent moisture conditions. Classification follows Perrone and Madramootoo (1998). a and b represent significant differences ($p < 0.05$) among the groups of API > 30 and API ≤ 30. ANOVA tests were confirmed by to Kolmogorov-Smirnov test and Normality plots with t-test.

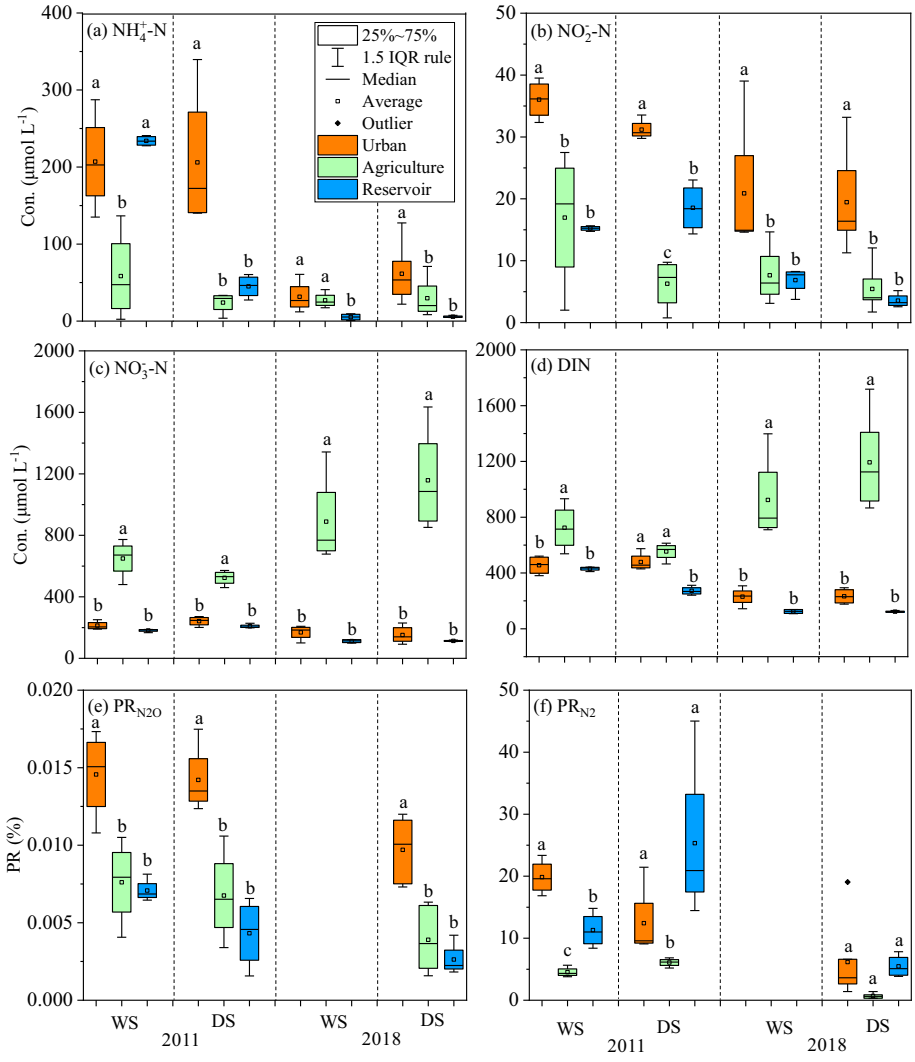

Fig. 5. Distribution of dissolved inorganic nitrogen concentrations, PR_{N2O} and PR_{N2} in 2011 and 2018. Data in 2011 were adapted from previous studies (Chen et al., 2015; Chen et al., 2014b). WS: wet season; DS: dry season.

*nxr*A, *nar*G and *nir*S, respectively ($p < 0.01$) (Fig. S3a), while in the dry season, only NO_3^--N, NO_2^--N and NH_4^+-N were correlated with *amo*A (AOA) and *nar*G ($p < 0.01$) (Fig. S3b). A stronger positive correlation between NO_3^--N and *nxr*A and *nir*S occurred in the wet season. NO_2^--N was positively correlated with *amo*A (AOB) ($p < 0.05$) in the wet season, while it was negatively correlated with *amo*A (AOA) ($p < 0.01$) in the dry season. A close relationship between NH_4^+-N and *nar*G was found in both the dry and wet seasons.

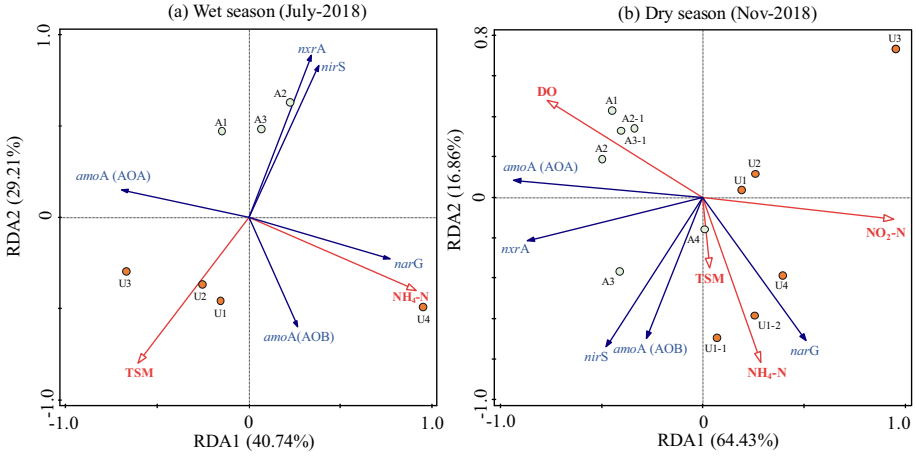

Fig. 6. RDA ordination plots indicate the relationship between the absolute abundance of functional genes and environmental factors among sampling sites.

4. Discussion

4.1. Anthropogenic nitrogen inputs influence nitrification and denitrification in river sections

The spatial variation of N concentration and composition reveals different anthropogenic source inputs to the urban and agriculture river sections (Fig. 5). As with previously reported values in the JR, NH_4^+-N derived from sewage (both raw and treated) was relatively more abundant in the urban river section, while NO_3^--N originating from ground water was dominant in the agriculture river section (Chen et al., 2015; Chen et al., 2014b). The higher N isotopes ($\delta^{15}N$) in the upper NJR (urban river section) suggest that Longyan city and suburban area produce a large amount of NH_4^+-N from manure and sewage disposal (Cao et al., 2015). Pinghe county in the upper WJR (agriculture river section) is known as "the town of Chinese pomelo" (Li et al., 2015), and excessive amounts of ammonia fertilizer have been applied to extensive areas of pomelo cultivation resulting in massive NO_3^--N pollution in groundwater and surface water (Chen et al., 2015; Guo et al., 2019) (Fig. 5c). It is clear that urban development and pomelo agriculture have markedly increased N loading and changed the concentration and composition of ammonium and nitrate in river water. Moreover, ammonium N decreased from 2011 to 2018 (Fig. 5a), following the nutrient abatement programs (e.g., upgrades to sewage treatment plant, reducing the number of livestock), and high flow years in 2015–2016 controlled by El Nino-Southern Oscillation.

The processing of ammonium N entering the fluvial system starts with ammonia oxidation. NH_4^+-N can be oxidized by ammonia-oxidizing microorganisms (AOB and AOA). AOB appears to play the primary role in the urban river section with a high concentration of NH_4^+-N compared to the agriculture river section (Fig. 2a). More relative abundance of *Nitrosomonas* (β-subclass AOB) was detected in the urban river section (Fig. 4b), which was likely retrieved from activated sludge and waste water discharge (Kowalchuk and Stephen, 2001; Rotthauwe et al., 1997). Wastewater from urban wastewater treatment plants (WWTPs), which has high levels of organic compounds with high metal complexation potentials, inhibits the growth of AOA (Gwak et al., 2020). In addition, AOB is better adapted to low DO concentrations than other nitrifiers in WWTPs due to the higher affinity of oxygen to AOB (Kauser et al., 2019; Soliman and Eldyasti, 2018). Unlike archaea, AOB might be more suited to high-ammonia, high-temperature, low-oxygen environments (Figs. 6, S3). As for the intermediate product of nitrification, nitrite accumulated in the urban river section (Fig. 5b), likely due to the lower nitrite transformation rate than ammonia oxidation. This is consistent with the result that *amo*A (AOB) was relatively more abundant than *nxr*A (NOB) in the urban river section (Fig. 2b). In addition, nitrite was positively correlated with NH_4^+-N (Fig. S3). As reported earlier, the *Nitrospira*-like NOB in wastewater treatment plants decreased with nitrite accumulation (Wrage et al., 2001), which was lower in water of the urban river section (Fig. 4b). AOB tends to reside in particle, but NOB tends to be more diffuse to resist oxygen limitation (Kowalchuk and Stephen, 2001). The fraction of particle-attached microbes of AOB (82%) was greater than NOB (74%) (Fig. 3). Nitrite accumulation could also occur during denitrification when the first step is more rapid than the second step, as *nar*G was more abundant than *nir*S in the urban river section (Fig. 2d). A previous study also reported that NO_2^--N was associated with partial nitrification and denitrification in sludge liquor (Stuven and Bock, 2001). Both denitrification (high abundance of *nar*G) and anammox (low abundance of *hzsB*) contributed to the production of N_2 in the urban river section (Table 1). The higher PR_{N2O} and PR_{N2} in the urban river section than the agriculture river section (Fig. 4e, f) and our recent study along Fujian coast (Lin et al., 2020) all suggest that urbanized river section became a hot spot of nitrification and denitrification. We concluded that high ammonium input favored the growth of nitrifier (AOB), and this enhanced nitrification and subsequent denitrification in the urban river section.

In the pomelo planting area (upper WJR), excess application of chemical fertilizers would cause significant nitrification in the vadose zone and down-leaching of nitrate to the groundwater as reported earlier (Dahan et al., 2014). A fairly high NO_3^--N concentration and DIN fraction as well as low pH was detected in the agriculture river section (Fig. 5c, Table S9), accompanied by a high AA and RA of *amo*A (AOA) and *nxr*A genes (Table 1). AOA was negatively correlated with NH_4^+-N (Fig. 6) and pH (Fig. S3). As an acido-neutrophilic microbe, AOA was expected to grow well under a medium NH_4^+-N, low pH environment (Ren et al., 2018). A relatively high abundance (13.7%) of *Nitrosotalea* cluster and the maximum OTUs of AOA were detected in water at site A3-1 (AW-1) next to orchard (Fig. 4a, c). *Nitrosotalea* was discovered and cultivated from acidic agricultural soil where ammonium availability was reduced by ionization (Lehtovirta-Morley et al., 2011). In addition, AOA in water was mostly present as particle-attached (PA) in the agriculture river section, likely associated with soil loss from river bank slope and uplands (Fig. 3a). There was a positive relationship between *nxr*A (NOB) abundance and DO in the agriculture river section with relative high DO level (Fig. S3). In contrast to the urban river section, less N_2O and N_2 production and more nitrate input resulted in a lower PR_{N2O} and PR_{N2} (Fig. 5e, f), corresponding to less *nar*G and more *hsz*B in the agriculture river section (Fig. 5e,f). We therefore speculated that complete nitrification by AOA and NOB and incomplete denitrification have enhanced nitrate accumulation in ground water, which occurred mainly in agricultural soil rather than in the river.

4.2. Hydroclimatic controls on nitrifiers and denitrifiers and gaseous nitrogen removal

In both the urban and agriculture river sections, the abundance of nitrifiers varied across seasons, likely associated with temperature and runoff. Higher TSM detected in the urban river section in the wet season favored the growth of particle-attached AOB (Table S9). Water temperature (30.5 ± 1.8 °C) in the wet season was within the optimum temperature range for nitrification (30–35 °C) (Hellinga et al., 1998). Nitrifiers had more AA and RA in the wet season than in the dry season, with the exception of AOA in the agriculture river section which was higher in the dry season (Table 1). Accordingly, nitrite and ΔN_2O, the intermediate product of nitrification, were higher in the wet season (Table S9). This is consistent with an earlier finding that increasing temperature would enhance nitrite accumulation when AOB outcompeted NOB (Bougard et al., 2006). The highest AA and RA of AOA were detected in the agriculture river section where the ratio of AOA/AOB was greater than one (Fig. 2a). The relationship of AOA absolute abundance with pH (negative) and with nitrate (positive) was most evident during the dry season (Fig. 6b). Previous studies suggest that AOA has a better tolerance to low pH soil than AOB (Gubry-Rangin et al., 2010), and a greater abundance of AOA was detected in the lower pH upstream of Qiantang River (Liu et al., 2013). The agriculture river section surrounded by acidic red soils had more relative abundance of *Nitrosotalea* (acidophilic cluster) (Fig. 4a). pH of river water would tend to be lower in the dry season than the wet season due to lower dilution of runoff (Table S9). In addition, decreasing pH was associated with nitrification as ammonium is oxidized to nitrite, releasing hydrogen ions (Eklind and Kirchmann, 2000). In summary, the optimum water temperature and turbid water in the wet season could promote the growth of nitrifiers and enhance nitrification in the urban river section, while lower pH favored AOA-driven nitrification in the agriculture river section.

The seasonal hydroclimatic influence on denitrifiers varied between the agriculture and urban river sections. There were larger AA and RA of denitrifiers (both *nar*G and *nir*S genes) in the wet season than in the dry season in the agriculture river section but no seasonal pattern was observed in the urban river section (Table 1). The optimum temperature for denitrifiers is 25–35 °C in pure cultures and soil (Braker et al., 2010), which was consistent with more denitrifiers observed in the

wet season (Table 1). In the wet season (urban river section), nitrite was higher (Fig. 5b) and had a positive relationship with *narG* (Fig. S3a), suggesting that the growth of denitrifier (*narG*) could favor the production of nitrite. In the dry season, more ammonium input (Fig. 4a) could enhance coupled nitrification-denitrification to support high denitrifier abundance (Table 3) in the urban river section, where the relationship between *narG* and ammonium was significantly positive (Fig. S3b). Therefore, denitrifier abundance (urban river section) was still high in the dry season though the temperature (24.1 °C) was lower than optimum (Table S1).

Gaseous N removal by nitrification and denitrification was higher in the wet season, and the high API period (due to higher rainfall) corresponded to the higher PR_{N2} and PR_{N2O}, especially in the urban river section (Fig. 5, Table 3). In the warm and wet season, stronger nitrification and denitrification and lower riverine ammonium and nitrate concentration together produced a higher PR_{N2} and PR_{N2O}. At the same time, higher rainfall increased runoff, carrying large amounts of TSM attached organic matter and ammonium, providing more potential sites for microbe growth and N transformations (Mohit et al., 2014). The majority of nitrifiers and denitrifiers were found to be attached to particulates (Fig. 3), which is consistent with studies in other aquatic systems (Fernandez-Gomez et al., 2013; Liu et al., 2019). In oxic running waters, the coupled nitrification-denitrification reactions can occur around suspended particles (Xia et al., 2017). Nevertheless, gene abundance was not significantly correlated with TSM, likely because the agriculture river section has less fine particles as the measurements of surface sediments indicate that most particles were coarse (Table S10). Anammox (*hzs*B) had higher RA in the wet season than in the dry season (Table 1). Overall, warm temperatures, high runoff and high TSM in the wet season promoted growth of nitrifiers, denitrifiers and anammox microbes, and as a result gaseous N retention increased.

4.3. Major factors controlling reservoir nitrification and denitrification and associated nitrogen retention by gaseous N removal

The AA of nitrifiers and denitrifiers in the reservoir was far lower than in the urban and agriculture river sections (Table 1). Mixing of water from external tributaries (Fig. 1) with the mainstream river reduced substrate (concentration of inorganic N species) in the reservoir for nitrification and denitrification (Fig. 5). The percentages of most functional genes of free-living (FL) AOA, AOB, denitrifiers and 16S rRNA in the reservoir were fairly high relative to other river sections (Fig. 3). As particle-attached (PA) microbes have higher energy requirements to attach themselves to particles and degrade organic matter, FL microbes usually dominate in oligotrophic waterbodies (Crespo et al., 2013; Ghiglione et al., 2009). As a result, lower nutrient and particle availability in the reservoir likely inhibited PA microbes but promoted the survival of FL nitrifiers and denitrifiers.

Reservoirs can reduce N loading by nitrification, denitrification and burial in sediments (Harrison et al., 2009), eliminating around 7% of N loading to the global river network (Akbarzadeh et al., 2019). In the dry season, both ΔN_2 and PR_{N2} in the reservoir section was higher while ΔN_2O and PR_{N2O} was lower than in the urban and agriculture river sections (Table S9). N_2O produced in reservoir with a longer water residence time could be likely further reduced to N_2 compared to N_2O in flowing water (Beaulieu et al., 2014). Grantz et al. (2012) observed a net denitrification occurred in sediments in contact with reservoir epilimnia during seasonal mixing, but net N_2 fixation occurred in these sediments during stratification. Denitrification was found to mainly occur in the sediment-water interface in a tropical reservoir (Upper Peirce Reservoir) and accounted for 98% of N_2 removal (Han et al., 2014). The retention of N_2 removal could also be related to anammox as there was a high RA of *hzs*B and particle-attached gene in the reservoir section (Table 1, Fig. 3f). The small-scale cascade dams in the NJR decrease minimum flow to generate electricity in the dry season (but do not decrease maximum flow in the wet season), reducing water velocity and suspended particles (Lu et al., 2018). Longer hydraulic retention time gives suspended particles more time to deposit, so reservoir TSM was lower than in the other river sections (Table S9). In addition, the lower water level in the dry season could aid N_2 diffusion from sediments to surface water. Gaseous N retention (ΔN_2 and ΔN_2O) and potential retention (PR_{N2} and PR_{N2O}) in the reservoir markedly declined from 2011 to 2018 (Fig. 5, Table S9), largely due to the reduction in N loading compared to the early 2010s (Chen et al., 2014a). Therefore, nitrification and denitrification in reservoir water were restricted by decreased N input, but sediment denitrification and anammox were expected to contribute more N retention, particularly in the dry season.

5. Conclusions

Microbe-driven nitrification and denitrification varied across river sections with different landscapes and anthropogenic N inputs. Urban sewage and intensive pomelo agriculture increased N concentrations and changed nutrient composition (ammonium versus nitrate) in river water. Discharge of urban sewage (both raw and treated) with high ammonium favored the growth of AOB (*Nitrosomonas* cluster) and enhanced N retention by denitrification in the urban river section. AOA had more abundance than AOB and high richness in the agriculture river section due to lower pH, low ammonium and high nitrate. Although the dominant AOA (*Nitrosotenuis* cluster) was comparable to the urban river section, higher relative abundance of acidophilic cluster (*Nitrosotalea*) was found in the agriculture river section. The lower PR_{N2O} and PR_{N2} suggest that nitrification and denitrification occurred mainly in agriculture soil rather than in the river. The seasonal pattern of measured parameters showed that warm temperatures, high runoff and high TSM in the wet season promoted growth of nitrifiers and denitrifiers and increased N retention by gaseous removal. One exception is that AOA-driven nitrification in the agriculture river section might be increased in the dry season due to lower pH. The reservoir section had relatively more FL nitrifiers and denitrifiers than river sites. Low nutrient and fewer particles in reservoir water reduced particle-attached microbes allowing free-living microbes to survive. Overall, nitrification and denitrification in reservoir water were not significant but denitrification and anammox occurring in sediments likely increased N retention (higher PR_{N2}), particularly in the dry season.

CRediT authorship contribution statement

Jingjie Lin: Writing - original draft. **Nengwang Chen:** Writing - review & editing. **Xin Yuan:** Data curation. **Qing Tian:** Data curation. **Anyi Hu:** Methodology. **Yi Zheng:** Software.

Declaration of competing interest

None.

Acknowledgements

This research was supported by the National Natural Science Foundation of China (No. 41676098; 51961125203). A. Hu acknowledges funding from the National Natural Science Foundation of China (31870475; U1805244). We thank all the students who assisted with fieldwork, Jonathan Vause for his assistance with English editing, and Xiuxiu Wang and Junou Du for their technical assistance.

Appendix A. Supplementary data

Supplementary data to this article can be found online at https://doi.org/10.1016/j.scitotenv.2020.141139.

References

Akbarzadeh, Z., Maavara, T., Slowinski, S., Van Cappellen, P., 2019. Effects of damming on river nitrogen fluxes: a global analysis. Glob. Biogeochem. Cycles 33, 1339–1357.

Akunna, J.C., Bizeau, C., Moletta, R., 1992. Denitrification in anaerobic digesters: possibilities and influence of wastewater COD/N-NOX ratio. Environ. Technol. 13, 825–836.

Arango, C.P., Tank, J.L., Schaller, J.L., Royer, T.V., Bernot, M.J., David, M.B., 2007. Benthic organic carbon influences denitrification in streams with high nitrate concentration. Freshw. Biol. 52, 1210–1222.

Beaulieu, J.J., Smolenski, R.L., Nietch, C.T., Townsend-Small, A., Elovitz, M.S., Schubauer-Berigan, J.P., 2014. Denitrification alternates between a source and sink of nitrous oxide in the hypolimnion of a thermally stratified reservoir. Limnol. Oceanogr. 59, 495–506.

Beusen, A.H.W., Bouwman, A.F., Van Beek, L.P.H., Mogollon, J.M., Middelburg, J.J., 2016. Global riverine N and P transport to ocean increased during the 20th century despite increased retention along the aquatic continuum. Biogeosciences 13, 2441–2451.

Bougard, D., Bernet, N., Cheneby, D., Delgenes, J.P., 2006. Nitrification of a high-strength wastewater in an inverse turbulent bed reactor: effect of temperature on nitrite accumulation. Process Biochem. 41, 106–113.

Bouwman, A.F., Bierkens, M.F.P., Griffioen, J., Hefting, M.M., Middelburg, J.J., Middelkoop, H., et al., 2013. Nutrient dynamics, transfer and retention along the aquatic continuum from land to ocean: towards integration of ecological and biogeochemical models. Biogeosciences 10, 1–22.

Braker, G., Schwarz, J., Conrad, R., 2010. Influence of temperature on the composition and activity of denitrifying soil communities. FEMS Microbiol. Ecol. 73, 134–148.

Cao, W.Z., Huang, Z., Zhai, W.D., Li, Y., Hong, H.S., 2015. Isotopic evidence on multiple sources of nitrogen in the northern Jiulong River, Southeast China. Estuar. Coast. Shelf Sci. 163, 37–43.

Chen, N.W., Hong, H.S., Zhang, L.P., Cao, W.Z., 2008. Nitrogen sources and exports in an agricultural watershed in Southeast China. Biogeochemistry 87, 169–179.

Chen, N.W., Chen, Z.H., Wu, Y.Q., Hu, A.Y., 2014a. Understanding gaseous nitrogen removal through direct measurement of dissolved N2 and N2O in a subtropical river-reservoir system. Ecol. Eng. 70, 56–67.

Chen, N.W., Wu, J.Z., Chen, Z.H., Lu, T., Wang, L.J., 2014b. Spatial-temporal variation of dissolved N2 and denitrification in an agricultural river network, southeast China. Agric. Ecosyst. Environ. 189, 1–10.

Chen, N.W., Wu, J.H., Zhou, X.P., Chen, Z.H., Lu, T., 2015. Riverine N2O production, emissions and export from a region dominated by agriculture in Southeast Asia (Jiulong River). Agric. Ecosyst. Environ. 208, 37–47.

Crespo, B.G., Pommier, T., Fernandez-Gomez, B., Pedros-Alio, C., 2013. Taxonomic composition of the particle-attached and free-living bacterial assemblages in the Northwest Mediterranean Sea analyzed by pyrosequencing of the 16S rRNA. Microbiologyopen 2, 541–552.

Crump, B.C., Armbrust, E.V., Baross, J.A., 1999. Phylogenetic analysis of particle-attached and free-living bacterial communities in the Columbia river, its estuary, and the adjacent coastal ocean. Appl. Environ. Microbiol. 65, 3192–3204.

Dahan, O., Babad, A., Lazarovitch, N., Russak, E.E., Kurtzman, D., 2014. Nitrate leaching from intensive organic farms to groundwater. Hydrol. Earth Syst. Sci. 18, 333–341.

Daims, H., Lucker, S., Wagner, M., 2016. A new perspective on microbes formerly known as nitrite-oxidizing bacteria. Trends Microbiol. 24, 699–712.

Dalsgaard, T., Canfield, D.E., Petersen, J., Thamdrup, B., Acuna-Gonzalez, J., 2003. N-2 production by the anammox reaction in the anoxic water column of Golfo Dulce, Costa Rica. Nature 422, 606–608.

Damashek, J., Smith, J.M., Mosier, A.C., Francis, C.A., 2015. Benthic ammonia oxidizers differ in community structure and biogeochemical potential across a riverine delta. Front. Microbiol. 5, 18.

Eklind, Y., Kirchmann, H., 2000. Composting and storage of organic household waste with different litter amendments. II: nitrogen turnover and losses. Bioresour. Technol. 74, 125–133.

Fernandez-Gomez, B., Richter, M., Schuler, M., Pinhassi, J., Acinas, S.G., Gonzalez, J.M., et al., 2013. Ecology of marine bacteroidetes: a comparative genomics approach. The ISME Journal 7, 1026–1037.

Galloway, J.N., Dentener, F.J., Capone, D.G., Boyer, E.W., Howarth, R.W., Seitzinger, S.P., et al., 2004. Nitrogen cycles: past, present, and future. Biogeochemistry 70, 153–226.

Gao, X.J., Chen, N.W., Yu, D., Wu, Y.Q., Huang, B.Q., 2018. Hydrological controls on nitrogen (ammonium versus nitrate) fluxes from river to coast in a subtropical region: observation and modeling. J. Environ. Manag. 213, 382–391.

Ghiglione, J.F., Conan, P., Pujo-Pay, M., 2009. Diversity of total and active free-living vs. particle-attached bacteria in the euphotic zone of the NW Mediterranean Sea. FEMS Microbiol. Lett. 299, 9–21.

Grantz, E.M., Kogo, A., Scott, J.T., 2012. Partitioning whole-lake denitrification using in situ dinitrogen gas accumulation and intact sediment core experiments. Limnol. Oceanogr. 57, 925–935.

Gubry-Rangin, C., Nicol, G.W., Prosser, J.I., 2010. Archaea rather than bacteria control nitrification in two agricultural acidic soils. FEMS Microbiol. Ecol. 74, 566–574.

Guo, J.X., Yang, J.C., Zhang, L.J., Chen, H.H., Jia, Y.M., Wang, Z., et al., 2019. Lower soil chemical quality of pomelo orchards compared with that of paddy and vegetable fields in acidic red soil hilly regions of southern China. J. Soils Sediments 19, 2752–2763.

Gwak, J.H., Jung, M.Y., Hong, H., Kim, J.G., Quan, Z.X., Reinfelder, J.R., et al., 2020. Archaeal nitrification is constrained by copper complexation with organic matter in municipal wastewater treatment plants. The ISME Journal 14, 335–346.

Hagy, J.D., Boynton, W.R., Keefe, C.W., Wood, K.V., 2004. Hypoxia in Chesapeake Bay, 1950–2001: long-term change in relation to nutrient loading and river flow. Estuaries 27, 634–658.

Han, H.J., Lu, X.X., Burger, D.F., Joshi, U.M., Zhang, L., 2014. Nitrogen dynamics at the sediment-water interface in a tropical reservoir. Ecol. Eng. 73, 146–153.

Harrison, J.A., Maranger, R.J., Alexander, R.B., Giblin, A.E., Jacinthe, P.A., Mayorga, E., et al., 2009. The regional and global significance of nitrogen removal in lakes and reservoirs. Biogeochemistry 93, 143–157.

He, X., Wu, J.P., Jiao, L.J., Wen, X.M., Wang, Y., Ou, L.J., et al., 2018. Development of a method for ammonia-oxidizing archaea diversity analysis based on amoA gene amplicons with high-throughput sequencing. Microbiology China 45, 1861–1870.

Hellinga, C., Schellen, A., Mulder, J.W., van Loosdrecht, M.C.M., Heijnen, J.J., 1998. The SHARON process: an innovative method for nitrogen removal from ammonium-rich waste water. Water Sci. Technol. 37, 135–142.

Hu, A.Y., Wang, H.J., Li, J.W., Liu, J., Chen, N.W., Yu, C.P., 2016. Archaeal community in a human-disturbed watershed in southeast China: diversity, distribution, and responses to environmental changes. Appl. Microbiol. Biotechnol. 100, 4685–4698.

Huang, S., Chen, C., Yang, X., Wu, Q., Zhang, R., 2011. Distribution of typical denitrifying functional genes and diversity of the nirS-encoding bacterial community related to environmental characteristics of river sediments. Biogeosciences 8, 3041–3051.

Inwood, S.E., Tank, J.L., Bernot, M.J., 2007. Factors controlling sediment denitrification in midwestern streams of varying land use. Microb. Ecol. 53, 247–258.

Johnson, L.T., Royer, T.V., Edgerton, J.M., Leff, L.G., 2012. Manipulation of the dissolved organic carbon pool in an agricultural stream: responses in microbial community structure, denitrification, and assimilatory nitrogen uptake. Ecosystems 15, 1027–1038.

Kauser, I., Ciesielski, M., Poretsky, R.S., 2019. Ultraviolet disinfection impacts the microbial community composition and function of treated wastewater effluent and the receiving urban river. PeerJ 7, 1–26.

Kowalchuk, G.A., Stephen, J.R., 2001. Ammonia-oxidizing bacteria: a model for molecular microbial ecology. Annu. Rev. Microbiol. 55, 485–529.

Kuypers, M.M.M., Sliekers, A.O., Lavik, G., Schmid, M., Jorgensen, B.B., Kuenen, J.G., et al., 2003. Anaerobic ammonium oxidation by anammox bacteria in the Black Sea. Nature 422, 608–611.

Lehtovirta-Morley, L.E., Stoecker, K., Vilcinskas, A., Prosser, J.I., Nicol, G.W., 2011. Cultivation of an obligate acidophilic ammonia oxidizer from a nitrifying acid soil. Proc. Natl. Acad. Sci. U. S. A. 108, 15892–15897.

Li, Y., Han, M.Q., Lin, F., Ten, Y., Lin, J., Zhu, D.H., et al., 2015. Soil chemical properties, 'Guanximiyou' pummelo leaf mineral nutrient status and fruit quality in the southern region of Fujian province, China. J. Soil Sci. Plant Nutr. 15, 615–628.

Liao, K.L.L., Bai, Y.H., Huo, Y., Jian, Z.Y., Hu, W.C., Zhao, C., et al., 2018. Integrating microbial biomass, composition and function to discern the level of anthropogenic activity in a river ecosystem. Environ. Int. 116, 147–155.

Lin, J.J., Chen, N.W., Wang, F.F., Huang, Z.Y., Zhang, X.Y., Liu, L., 2020. Urbanization increased river nitrogen export to western Taiwan Strait despite increased retention by nitrification and denitrification. Ecol. Indic. 109, 1–10.

Liu, Z.H., Huang, S.B., Sun, G.P., Xu, Z.C., Xu, M.Y., 2011. Diversity and abundance of ammonia-oxidizing archaea in the Dongjiang River, China. Microbiol. Res. 166, 337–345.

Liu, S., Shen, L.D., Lou, L.P., Tian, G.M., Zheng, P., Hu, B.L., 2013. Spatial distribution and factors shaping the niche segregation of ammonia-oxidizing microorganisms in the Qiantang River, China. Appl. Environ. Microbiol. 79, 4065–4071.

Liu, K.S., Hou, J.Z., Liu, Y.Q., Hu, A.Y., Wang, M.D., Wang, F., et al., 2019. Biogeography of the free-living and particle-attached bacteria in Tibetan lakes. FEMS Microbiol. Ecol. 95, 10.

Lu, W.W., Lei, H.M., Yang, D.W., Tang, L.H., Miao, Q.H., 2018. Quantifying the impacts of small dam construction on hydrological alterations in the Jiulong River basin of Southeast China. J. Hydrol. 567, 382–392.

Lv, P., Luo, J., Zhuang, X., Zhang, D., Huang, Z., Bai, Z., 2017. Diversity of culturable aerobic denitrifying bacteria in the sediment, water and biofilms in Liangshui River of Beijing, China. Sci. Rep. 7, 10032.

Maloney, K.O., Weller, D.E., 2011. Anthropogenic disturbance and streams: land use and land-use change affect stream ecosystems via multiple pathways. Freshw. Biol. 56, 611–626.

Mohit, V., Archambault, P., Toupoint, N., Lovejoy, C., 2014. Phylogenetic differences in attached and free-living bacterial communities in a temperate coastal lagoon during summer, revealed via high-throughput 16S rRNA gene sequencing. Appl. Environ. Microbiol. 80, 2071–2083.

Perrone, J., Madramootoo, C.A., 1998. Improved curve number selection for runoff prediction. Can. J. Civ. Eng. 25, 728–734.

Ren, L.H., Cai, C.Q., Zhang, J.C., Yang, Y., Wu, G.Y., Luo, L., et al., 2018. Key environmental factors to variation of ammonia-oxidizing archaea community and potential ammonia oxidation rate during agricultural waste composting. Bioresour. Technol. 270, 278–285.

Rotthauwe, J.H., Witzel, K.P., Liesack, W., 1997. The ammonia monooxygenase structural gene amoA as a functional marker: molecular fine-scale analysis of natural ammonia-oxidizing populations. Appl. Environ. Microbiol. 63, 4704–4712.

Schloss, P.D., Westcott, S.L., Ryabin, T., Hall, J.R., Hartmann, M., Hollister, E.B., et al., 2009. Introducing mothur: open-source, platform-independent, community-supported software for describing and comparing microbial communities. Appl. Environ. Microbiol. 75, 7537–7541.

Soliman, M., Eldyasti, A., 2018. Ammonia-oxidizing bacteria (AOB): opportunities and applications-a review. Rev. Environ. Sci. Biotechnol. 17, 285–321.

Strous, M., vanGerven, E., Kuenen, J.G., Jetten, M., 1997. Effects of aerobic and microaerobic conditions on anaerobic ammonium-oxidizing (Anammox) sludge. Appl. Environ. Microbiol. 63, 2446–2448.

Stuven, R., Bock, E., 2001. Nitrification and denitrification as a source for NO and NO2 production in high-strength wastewater. Water Res. 35, 1905–1914.

Weiss, R.F., 1970. The solubility of nitrogen, oxygen and argon in water and seawater. Deep-Sea Res. Oceanogr. Abstr. 17, 721–735.

Weiss, R.F., Price, B.A., 1980. Nitrous-oxide solubility in water and seawater. Mar. Chem. 8, 347–359.

Wrage, N., Velthof, G.L., van Beusichem, M.L., Oenema, O., 2001. Role of nitrifier denitrification in the production of nitrous oxide. Soil Biol. Biochem. 33, 1723–1732.

Xia, X.H., Liu, T., Yang, Z.F., Michalski, G., Liu, S.D., Jia, Z.M., et al., 2017. Enhanced nitrogen loss from rivers through coupled nitrification-denitrification caused by suspended sediment. Sci. Total Environ. 579, 47–59.

Yang, S.Z., Liebner, S., Alawi, M., Ebenhoh, O., Wagner, D., 2014. Taxonomic database and cut-off value for processing mcrA gene 454 pyrosequencing data by MOTHUR. J. Microbiol. Methods 103, 3–5.

Yang, J., Feng, L., Pi, S., Cui, D., Ma, F., H-p, Zhao, et al., 2020. A critical review of aerobic denitrification: insights into the intracellular electron transfer. Sci. Total Environ. 731, 139080.

Yu, D., Yan, W.J., Chen, N.W., Peng, B.R., Hong, H.S., Zhuo, G.H., 2015. Modeling increased riverine nitrogen export: source tracking and integrated watershed-coast management. Mar. Pollut. Bull. 101, 642–652.

Yu, C., Huang, X., Chen, H., Godfray, H.C.J., Wright, J.S., Hall, J.W., et al., 2019a. Managing nitrogen to restore water quality in China. Nature 567, 516–520.

Yu, D., Chen, N.W., Krom, M.D., Lin, J.J., Cheng, P., Yu, F.L., et al., 2019b. Understanding how estuarine hydrology controls ammonium and other inorganic nitrogen concentrations and fluxes through the subtropical Jiulong River Estuary, SE China under baseflow and flood-affected conditions. Biogeochemistry 142, 443–466.

Zhang, X., Gu, Q., Long, X.E., Li, Z.L., Liu, D.X., Ye, D.H., et al., 2016. Anthropogenic activities drive the microbial community and its function in urban river sediment. J. Soils Sediments 16, 716–725.

Zheng, B.X., Zhu, Y.G., Sardans, J., Penuelas, J., Su, J.Q., 2018. QMEC: a tool for high-throughput quantitative assessment of microbial functional potential in C, N, P, and S biogeochemical cycling. Science China-Life Sciences 61, 1451–1462.

Zhou, L., Wang, S., Zou, Y., Xia, C., Zhu, G., 2015. Species, abundance and function of ammonia-oxidizing archaea in inland waters across China. Sci. Rep. 5, 15969.

Zhou, X., Chen, N., Yan, Z., Duan, S., 2016. Warming increases nutrient mobilization and gaseous nitrogen removal from sediments across cascade reservoirs. Environ. Pollut. 219, 490–500.